INTERACTIVE CONTROL ENGINEERING
Principles and Applications

Volume 7 Nonlinear Dynamics, Oscillations, and Stabilization

CHAPTER 12

Input Shaping on an Overhead Crane Where One Actuator Serves Two Outputs

Pages 288–314

Edited by John D. Hedengren

How to cite this chapter. "Input Shaping on an Overhead Crane Where One Actuator Serves Two Outputs," in *Nonlinear Dynamics, Oscillations, and Stabilization*, John D. Hedengren, Ed., vol. 7 of *Interactive Control Engineering: Principles and Applications*. Advanced Process Solutions, LLC, 2026, ch. 12, pp. 288–314.

The page numbers in this file are those of the printed volume.

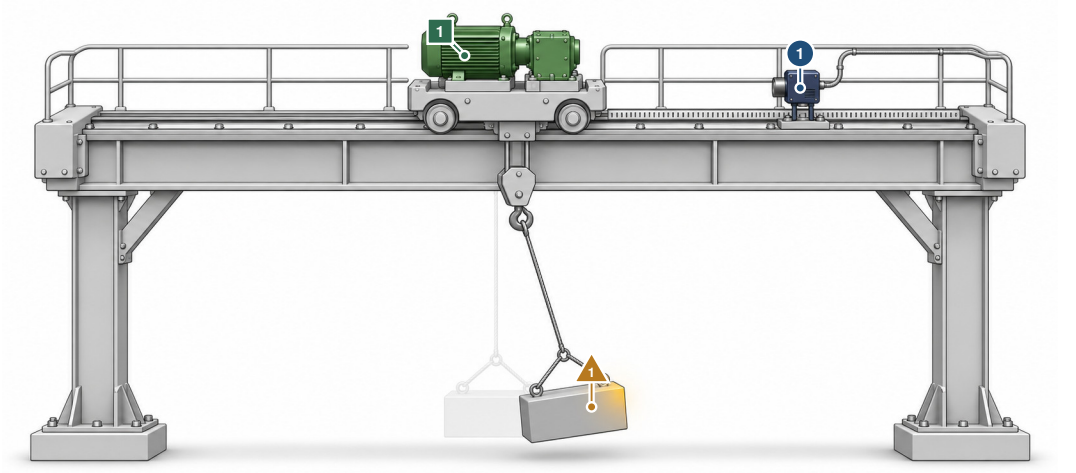
The app for this chapter
https://apmonitor.com/apps/overhead-crane/

The volume online: contents, other chapters and citation records
https://apmonitor.com/apps/books/v07-nonlinear-stabilization/#overhead-crane

Copyright © 2026 Advanced Process Solutions, LLC. All rights reserved. Produced by Advanced Process Solutions, LLC.

CHAPTER 12

Input Shaping on an Overhead Crane Where One Actuator Serves Two Outputs



The controller moves 1 trolley travel drive

The controller reads 1 trolley position

What disturbs it 1 hoist pay-out, payload mass and wind on the load

One drive moves the trolley, only its position is read, and the timing of each move decides whether the hanging load arrives swinging or still. Illustration, not to scale.

IN PLAIN TERMS **Moving a Crane Without Setting the Load Swinging**

The main idea. A crane trolley rolls along a beam with a load hanging from a cable below it. One motor must stop the trolley over its target and leave the load still. Nothing measures the swing.

The challenge. A quick move sets the load swinging like a pendulum, and the swing barely dies away. Splitting each move into a few timed pieces lets the later pieces cancel the swing the first one started. The timing must match the length of the cable.

Why it matters. Every second spent waiting for a load to stop swinging is lost again on every lift the crane makes.

THREE WAYS TO READ THIS CHAPTER

Explore	12 min	the first page, the fact in the Introduction (Section 12.1), the history in Section 12.2, the fact and the try-its in Section 12.6, and the key points
Study	55 min	the whole chapter with its three pause points and the twelve exercises at its end
Practice	20 min	the first page, the results (Section 12.6), Technology in Practice (Section 12.7), Limitations (Section 12.8) and the open challenge

The control question One drive on a gantry crane trolley has to park the trolley and leave the hanging load still, and no controller reads the swing. How much sway does a shaped command remove, what does it lose when its assumed cable length or the drive rating is wrong, and how does a predictive controller on the same model compare?

Learning objectives

- Derive the trolley and payload balances, and explain why a sudden push accelerates the trolley at F/M.
- Compute the impulse amplitudes and times of the ZV and ZVD shapers from an assumed cable length and damping ratio.
- Estimate the residual sway of a mistuned shaper from the ratio of true to design frequency, including the coupled mode of the closed loop.
- Show from runs why shaping fails on a saturated drive and on sway that is already present.
- Commission a crane move in the order damping, gain, shaping.

Prerequisites Sections 1.4.1 (the hanging cart), 1.4.4 (eigenvalues), 1.4.8 (input shaping) and 1.6.2 (velocity form). Section 1.6.3 is needed only for the predictive controller. Chapter 7 for a pendulum moved by its cart.

The app https://apmonitor.com/apps/overhead-crane/

See also Volume 3, Chapter 12 for two-impulse and three-impulse shapers on a ribbon mode under a speed loop. Volume 9, Chapter 4 for an offset-free MPC whose Kalman filter carries a disturbance state, and Volume 9, Chapter 12 for a point-to-point move planned by optimal control.

12.1 Introduction

A control problem is normally posed with one actuator behind every quantity that has to be held somewhere. A gantry crane does not offer that arrangement. The trolley carries one drive, the operator requires both that the trolley stop at a target and that the load beneath it be still when it arrives, and the swing angle has no actuator attached to it at all. The swing is excited or canceled only through the history of the trolley acceleration, which is the same signal the position loop is using for its own purpose. The plant carries four mechanical states, one input and two outputs of interest. Chapter 11 meets the same arrangement in a strut that pushes the body and the wheel with one force.

The system is not an inverted pendulum. The load hangs below the trolley and requires no balancing, unlike the upright pole of Chapter 7, which also responds only to the acceleration of its cart. It is the hanging cart of Section 1.4.1. The difficulty is that the load is a resonator with almost no damping, at a frequency $\omega_n = \sqrt{g/\ell}$ that a hoist changes every time it runs, and a point-to-point move whose duration is a few multiples of the swing period excites it strongly. On the default configuration of the application, a 6 m move that parks the trolley inside ± 0.10 m at 9.88 s leaves the payload swinging with an amplitude of 7.87°, and the swing is still 2.81° at $t = 20$ s. The position loop meets its own specification. It has no access to the quantity that is still moving.

Two remedies exist and they are structurally different. The first adds a sensor and closes a second loop around the angle, which is what a nonlinear coupling controller or a state-feedback anti-sway system does. The second leaves the loop untouched and changes what the loop is asked for, convolving the reference with a short train of impulses chosen so that the vibration the later impulses start cancels the vibration the earlier ones left. Command shaping is feedforward in the strict sense. It costs nothing in stability margin, it can be retrofitted to a crane whose drive controller is a sealed box, and it carries a specific and testable weakness, because a canceler tuned to the wrong frequency does not cancel. The absence of an angle measurement is a property of the instrumentation rather than of the machine, and it is what makes command shaping the appropriate tool on this apparatus, because a mistuned shaper announces itself only through the residual sway it leaves behind.

The experiments of this chapter isolate a specific set of process dynamics and control principles. The plant is underactuated, so the count of independent actuators against the count of regulated outputs decides what feedback can reach, and the residual sway is the part of the response no gain

touches. Command shaping separates feedforward action on the reference from feedback action on the error, because the impulse train changes the setpoint the loop follows and leaves every controller coefficient alone. Resonance, damping ratio and the sensitivity of a canceler to a frequency error become measurable rather than asserted. Actuator saturation is a failure class distinct from poor tuning, because a drive resting on its limit no longer follows the command it was given. The physical fundamentals are a horizontal momentum balance on the trolley and a moment balance on the suspended load, coupled through the cable tension, together with the time-scale separation between a position loop that has to be slow and a payload resonance that is not. Those are the same conservation principles and the same loop structures that govern process applications built on material and energy balances [1–3], in a setting where the geometry is directly observable. The behavior matters industrially because sway is paid for in the seconds an operator spends waiting for a load to settle, on every cycle of a machine whose cycle time sets the throughput of the facility around it.

> ✦ **DID YOU KNOW? Waiting for the Load at a Container Quay**
>
> On ship-to-shore cranes without anti-sway, the operator waits on average about 15 s for the load to settle at each end of a move. At about 19 containers an hour per crane, anti-sway was estimated to add about two [4].

Textbook accounts of input shaping give the impulse amplitudes and a sensitivity curve and then move on to an application example [5]. A printed sensitivity curve does not quantify what the same shaper loses when four meters of cable are paid out, what a longer shaper recovers, or what neither of them can repair once the drive is on its limit. This chapter puts numbers on what command shaping is worth on a simulated overhead crane as the cable length, the payload mass, the drive rating and the origin of the sway are changed one at a time. Input shaping and the crane model are both established, and the numbers are the subject.

Section 12.2 traces the problem from the crane operator's timed two-pulse command to the robust shapers. Section 12.3 carries every relation and every constant needed to rebuild the plant: its state equations, parameter values, hard limits and sample periods. Section 12.4 shows that the frequency a shaper on this machine ought to be tuned to is not $\sqrt{g/\ell}$ at all but the coupled mode of trolley and payload with the position loop closed. A fifth-order linearization reproduces that mode to within 0.1 % of the period timed in the simulator at three separate configurations, names the assumed cable length that minimizes residual sway to the 0.25 m resolution of a measured sweep, and accounts for the position loop damping the payload four times faster than the cable pivot manages on its own. The same section derives the two shapers and their sensitivity to a frequency error. Section 12.5 gives the discrete algorithm the controller executes and a model predictive controller given the shaper's cable length. Section 12.6 scores thirteen configurations on the numbers the application computes while it runs, and sets the predictive controller against the shapers in Section 12.6.5. Section 12.7 describes the sensors, drives and controllers of real cranes, Section 12.8 states the limitations and Section 12.9 concludes.

12.2 Background

Crane operators solved this problem by hand long before it was written down. A skilled driver of a bridge crane accelerates, coasts, and then decelerates at a moment chosen so that the load arrives over the target with the cable vertical, which is a two-pulse command timed against the pendulum period and is exactly the maneuver an automatic shaper performs. The cost of doing it by eye is that the operator must watch the load rather than the destination, and that every new load, every new cable length and every new driver produces a different result.

The control formulation arrived from a different direction, from Posicast control to the robust shapers, as the history segment below tells. Direct comparison of the robust shapers on common ground establishes what each one costs in delay [6].

> ⧖ HISTORY **From Posicast to Robust Shapers, 1957 to 1994**
>
> Posicast control, published in 1957, removed the ringing of a lightly damped feedback system by exciting several transient oscillations at closely spaced times, with magnitudes and phases chosen so that their sum is zero. Split into two spaced excitations, a step settled in one half cycle, and in an electrical feedback system the extra hardware was one or two artificial transmission lines [7]. Preshaped command inputs, published in 1990, completed a move without residual vibration for a time penalty on the order of one period of the first mode. They were robust to parameter uncertainty, could be applied open or closed loop, and cut the residual vibration of a simulator of the Space Shuttle's robot arm by a factor of 25 [8]. A vector-diagram method of 1994 needed only estimates of the frequency and the damping, and given a bound on the acceptable residual it chose a shaper insensitive to frequency errors [9].

Cranes became the standard test case for the method. Modeling and control of cranes has its own review literature, covering gantry, bridge, boom and tower configurations, the planar and three-dimensional models, and the split between open-loop and closed-loop approaches [10, 11]. Hoisting during a traverse is the difficult case, because the natural frequency sweeps while the shaper runs, and measurements on an industrial gantry quantify what a fixed shaper loses and what recomputing the impulse train from a live cable length recovers [12]. Volume 3, Chapter 12 applies two-impulse and three-impulse shapers to a structural mode of a ribbon under a climber. Combining a shaper on the command path with a positioning loop, so that a crane both parks accurately and arrives quiet, has been demonstrated on production bridge and gantry machines [13]. The closed-loop alternative develops in parallel, with nonlinear coupling laws that feed the swing angle back into the trolley force and prove asymptotic regulation of both coordinates [14], and the general problem of controlling a mechanical system with fewer actuators than degrees of freedom has become a field of its own [15].

The economic motive is throughput. A container terminal is a queue of ship-to-shore and yard cranes whose cycle time sets the berth productivity of the whole facility, and the operations research literature on terminal design treats crane cycle time as the primary resource [16]. Sway lengthens that cycle, because an operator who cannot rely on the load being still must slow down, wait, or make a correcting move. Controlled experiments with human operators driving an instrumented bridge crane through an obstacle course, with input shaping switched on and off, report faster and safer completion with shaping enabled [17]. The improvement is not confined to the machine, because the operator no longer has to compensate for the swing.

12.3 Crane Model

The simulated machine is a single trolley on a horizontal rail with one point-mass payload hanging beneath it on one cable, confined to the vertical plane that contains the rail. Figure 12.1 collects the geometry, the five states, the drive force, the three disturbances and the one instrument.

12.3.1 Signal Classification and Ranges

Two variables are declared as controlled variables and the shipped controller regulates only one of them. The trolley position is held against an operator setpoint by the single feedback loop of that controller. The swing angle is declared with a setpoint of 0° and a band of 0.5° so that it is trended and scored beside the position loop, and the shipped controller never reads it. The same drive force is reported under both, because one actuator serves both. Table 12.1 sorts each signal by the part it plays and gives the interval over which the application allows it to move.

12.3.2 Equations of Motion

The trolley obeys a horizontal momentum balance in which the payload pushes back through the cable, and the payload obeys a moment balance about the suspension point, already divided through by $m\ell$. They are given in Equation (12.1).

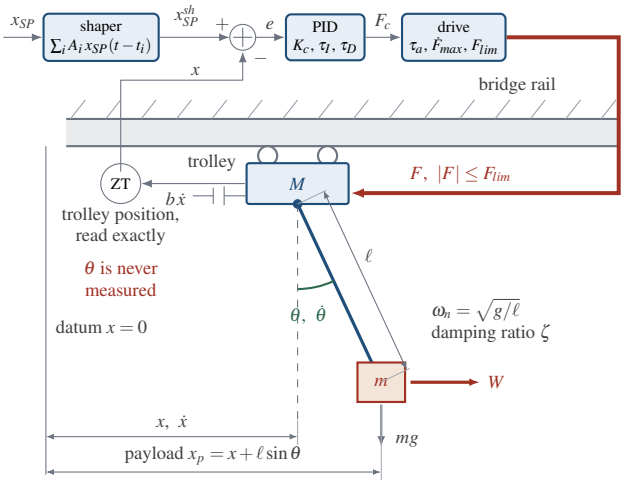


Figure 12.1 Overhead crane geometry with the command path drawn above it. Each symbol appearing in the two balances, in the impulse train and in the control law is labeled. The trolley position is the only instrument the shaped loop reads, and no path whatever leads from the swing angle back to the drive through that loop.

Table 12.1 Signals, Their Roles and Their Ranges

Symbol	Role	Unit	Range or default
x	CV, position loop	m	setpoint 0 to 24, band ± 0.10
θ	CV, MPC objective only	deg	setpoint 0, band ± 0.5
F	MV, position loop	N	$\lvert F\rvert \le F_{lim}$
x	state, trolley position	m	free
$\dot{x}$	state, trolley velocity	m/s	free
θ	state, swing angle	rad	$\lvert\theta\rvert \le \theta_{lim}$
$\dot{\theta}$	state, swing rate	rad/s	free
F	state, force developed	N	$\lvert F\rvert \le F_{lim}$
$\Delta\ell$	DV, hoist paid out	m	-2.5 to $+8$, default 0
Δm	DV, payload mass change	%	-60 to $+150$, default 0
W	DV, wind on the payload	N	-250 to $+250$, default 0
$\Delta\dot{\theta}$	DV, bump event	rad/s	$+0.09$
$\Delta\dot{\theta}$	DV, gust event	rad/s	-0.14
$\Delta\ell$	DV, pay-out event	m	$+2$, capped at $+8$
f_{man}	operator actuator	N	-4000 to $+4000$
θ_m	measurement, MPC option	deg	off by default
ℓ_a	shaper design length	m	1.5 to 12, default 4.00
ζ_a	shaper design damping	—	0 to 0.100, default 0.015

$$\begin{aligned}(M+m)\ddot{x} + m\ell\ddot{\theta}\cos\theta - m\ell\dot{\theta}^2\sin\theta + b\dot{x} &= F + W,\\ \ell\ddot{\theta} + \ddot{x}\cos\theta + g\sin\theta + 2\zeta\omega_n\ell\dot{\theta} &= \frac{W}{m}\cos\theta\end{aligned} \tag{12.1}$$

where M is the trolley mass, m the payload mass, ℓ the cable length in use, b the lumped rail and gearbox friction coefficient, ζ the sway damping ratio, g the gravitational acceleration, F the force the drive has developed and W a horizontal wind force on the payload. The payload hangs at $(x + \ell\sin\theta,\ -\ell\cos\theta)$ relative to the trolley, so a positive θ means the load is ahead of the trolley in the $+x$ direction, and a forward push therefore drives θ negative. The wind appears in both balances

because the payload can move both by the trolley translating and by the cable swinging, and its generalized forces are $Q_x = W$ and $Q_\theta = W\ell\cos\theta$. The last term of the second relation is written as $2\zeta\omega_n\ell\dot\theta$ so that ζ is the payload damping ratio directly, which is the number the shaper formulas need.

The coupling is not linearized. The two accelerations are collected on the left and solved as the two-by-two system of Equation (12.2) at every right-hand-side evaluation.

$$\begin{bmatrix} M+m & m\ell c \\ c & \ell \end{bmatrix} \begin{bmatrix} \ddot x \\ \ddot\theta \end{bmatrix} = \begin{bmatrix} F + W + m\ell\dot\theta^2 s - b\dot x \\ -gs - 2\zeta\omega_n\ell\dot\theta + (W/m)c \end{bmatrix} \tag{12.2}$$

where $s = \sin\theta$ and $c = \cos\theta$ have been abbreviated to keep the display inside the column.

The determinant is $\ell(M + m\sin^2\theta)$, which is strictly positive for any physical cable length, so the solve is unconditionally well posed. The solution at $\theta = 0$ states the character of the plant. The trolley acceleration is F/M, not $F/(M+m)$. A load on the end of a cable cannot resist a sudden push and contributes nothing to the trolley inertia until it has started to swing, and it is only at low frequency, where the payload follows the trolley, that the combined mass $M+m$ is the right one.

Pause. Try Exercise 12.2 before reading on.

The drive is a force source with a first-order lag, and the force it is commanded to produce is rate limited twice, once inside the controller and again on the applied command, as shown in Equation (12.3).

$$\begin{aligned} \tau_a\dot F &= F_a - F, \qquad |\dot F_a| \le \dot F_{max}, \\ F_{lim} &= \min\bigl(F_{max},\,(M+m)\,a_{max}\bigr) \end{aligned} \tag{12.3}$$

where τ_a is the drive time constant, F_a the applied command and $\dot F_{max}$ the slew limit. At the default parameters $(M+m)a_{max} = 1350\times 4.0 = 5400\,\mathrm{N}$ exceeds the motor rating, so $F_{lim} = F_{max} = 4000\,\mathrm{N}$ and the acceleration limit is inactive until a scenario derates the drive or a heavy payload is hung on it.

The natural frequency and period of the suspended load, and the damped frequency the shaper timings use, are given by Equation (12.4).

$$\omega_n = \sqrt{\frac{g}{\ell}}, \qquad T_n = 2\pi\sqrt{\frac{\ell}{g}}, \qquad \omega_d = \omega_n\sqrt{1-\zeta^2} \tag{12.4}$$

Neither mass appears. At the default 4.00 m cable this is $\omega_n = 1.5660\,\mathrm{rad/s}$ and $T_n = 4.012\,\mathrm{s}$, and because $\zeta = 0.015$ the damped and undamped frequencies differ by 0.011 %. The damping enters the shaper almost entirely through the impulse amplitudes and hardly at all through the impulse timings.

The instantaneous sway amplitude reported by the application is the phase-plane radius of Equation (12.5).

$$A = \sqrt{\theta^2 + \left(\frac{\dot\theta}{\omega_n}\right)^2} \tag{12.5}$$

For free oscillation $\theta = A\sin(\omega_n t + \phi)$ this is exact at every instant, so the amplitude is readable the moment a move ends rather than after a further full period, which is what makes a residual-sway number meaningful on a run that lasts only a few periods.

12.3.3 Parameters, Limits and Numerics

Every constant the simulation uses anywhere appears in Table 12.2, grouped as the plant, the drive, the loop with its shaper and the predictive controller, the limits and alarms, and the numerics, except the fixed decision period, weights, prices and noise variances of the predictive controller, which

Table 12.2 Every Constant in the Crane Simulation and Its Adjustable Range

Symbol	Meaning	Value	Adjustable range
M	trolley mass	1200 kg	400 to 3000
m	payload mass, nominal	150 kg	25 to 800
ℓ	cable length, nominal	4.00 m	1.5 to 12
b	trolley damping	400 N s/m	0 to 1500
ζ	sway damping ratio	0.015	0 to 0.100
g	gravity	9.81 m/s^2	1.6 to 24.8
F_{max}	drive rating	4000 N	400 to 4000
a_{max}	acceleration limit	4.0 m/s^2	0.3 to 6.0
$\dot{F}_{max}$	force slew limit	12 000 N/s	1000 to 40000
τ_a	drive time constant	0.08 s	0 to 0.40
F_{push}	manual push force (hidden)	2400 N	200 to 4000
t_{push}	manual push duration (hidden)	0.8 s	0.1 to 3.0
K_c	position loop gain	620 N/m	40 to 1800
τ_I	integral time	1000 s	5 to 2000
τ_D	derivative time	2.3 s	0 to 6
τ_f	derivative filter	0.02 s	0 to 0.50
ℓ_a	shaper design length	4.00 m	1.5 to 12
ζ_a	shaper design damping	0.015	0 to 0.100
T_p	MPC prediction horizon	6 s	2 to 10
θ_{max}	MPC swing limit	3°	0.5 to 15
x_{max}	MPC travel limit	24 m	1 to 24
x_{tol}	parked tolerance	0.10 m	0.02 to 0.50
θ_{ok}	quiet-sway threshold	0.5°	0.1 to 3.0
θ_{alarm}	excessive-sway alarm	12°	3 to 40
θ_{lim}	cable slack limit (hidden)	1.4 rad	0.5 to 1.5
Δt	integration step (RK4)	0.005 s	fixed
Δt_c	control period	0.01 s	fixed
f_{log}	historian rate	50 Hz	fixed
N_h	setpoint history depth	4096 samples	fixed

The setpoint history holds 40.96 s at the control rate, against a longest shaper span of 6.95 s at the 12 m maximum cable. Random draws are seeded at 20260824, although no scenario in this application injects noise.

are given with its design in Section 12.5.4. Three of them are not exposed for adjustment in the application. One of the three, the swing limit, halts the integration of an unphysical angle rather than continuing to simulate a cable that has gone slack.

The engine of Section 1.6.1 integrates the five states on a fixed 5 ms grid, roughly 800 steps per swing period at the default cable length. Control runs at 100 Hz, the rate a crane drive programmable logic controller would use, on every second step, and the historian samples at 50 Hz. Scheduled events run first in a step, so a setpoint step scheduled at 1.5 s reaches the controller scan at 1.5 s. The post-step block holds θ at θ_{lim} with $\dot{\theta}$ set to zero and raises a swing-limit fault when the angle exceeds 1.4 rad, clearing again at 90 % of that value, sets the developed force equal to F_a when τ_a is set to zero, evaluates Equation (12.5), tests $|x - x_{SP}| \le x_{tol}$ against the *raw* setpoint rather than the shaped one, and updates the residual-sway statistic only while that test passes. Every scenario initializes the trolley parked at its setpoint with the drive idle and, except configuration 9, the cable vertical, so the crane starts in an exact equilibrium and every move in the application is a genuine setpoint change for the shaper to act on.

The cable length in use is $\ell = \mathrm{clamp}(\ell_0 + \Delta\ell, 0.4, 24)$ and the payload mass in use is $m = m_0(1 + \Delta m/100)$, so the hoist disturbance changes the resonance and the mass disturbance does not.

12.3.4 Assumptions

Point mass on a rigid, massless, always taut cable. A real hook block and sling is a double pendulum with a second and faster mode that no single-mode shaper touches, and control of the double-pendulum case needs a shaper designed for two frequencies at once. Cable stretch, load rotation and the inertia of the load about its own center are all absent.

Constant cable length during a move. Cranes hoist and traverse at the same time, which sweeps the natural frequency continuously and defeats any fixed impulse train. The hoist here is a disturbance that steps between moves rather than a second axis running concurrently, and the measured penalty for a fixed shaper under a real hoisting profile is larger than anything reported below [12].

Planar motion. The bridge axis at right angles to the trolley axis, the out-of-plane sway mode it excites and the interaction between the two are all omitted, as is any wind component across the rail.

Linear viscous sway damping. The loss term is $2\zeta\omega_n\ell\dot{\theta}$ with $\zeta = 0.015$, which gives an amplitude decay time of $1/(\zeta\omega_n) = 42.6\,\mathrm{s}$ at 4 m with the trolley held. Real losses are dominated by aerodynamic drag and grow faster than linearly with swing rate, so the model overstates how long a large swing persists and understates how long a small one does.

An idealized drive. The force path is a rating, a slew limit and a first-order lag. There is no gearbox backlash, no torque ripple, no stiction and no breakaway friction, and because the rail loss is a single viscous coefficient the trolley creeps for any nonzero force.

Perfect position and no angle measurement. The trolley position is read exactly, with no noise, bias, quantization or delay, and the swing angle is not instrumented at all unless the optional sensor of the predictive controller is switched on, which reads it just as exactly. The second half of that is a modeling choice rather than a limitation, and it is the point of the chapter. Adding an angle measurement changes the problem from command shaping to genuine anti-sway feedback [14].

The fixed-pivot formula is an approximation. Equation (12.4) is the frequency of a pendulum on a rigid pivot. The trolley is not rigid, which Section 12.4 quantifies.

12.4 Dynamic Analysis

12.4.1 Position Loop Bandwidth

With the payload following the trolley at low frequency and the derivative action supplying the only damping the loop has, the position loop is the second-order system of Equation (12.6).

$$\omega_c = \sqrt{\frac{K_c}{M+m}}, \qquad \zeta_c = \frac{b + K_c\tau_D}{2\sqrt{K_c(M+m)}} \tag{12.6}$$

At the default tuning this places the loop at $\omega_c = 0.678\,\mathrm{rad/s}$ with $\zeta_c = 1.00$, which is well damped and, more to the point, a factor of 2.3 slower than the payload resonance at 1.566 rad/s. That separation is deliberate. Placing the loop at twice the sway frequency would need $K_c = 4\omega_n^2(M+m) = 13.2\,\mathrm{kN/m}$ and a 6 m step would then ask the drive for 79 kN against a 4 kN rating. The gap between the achievable loop bandwidth and the payload resonance is the reason command shaping exists on this plant. The swing is not removed by raising the gain.

Integral action is effectively disabled at the default $\tau_I = 1000\,\mathrm{s}$, because the plant has no steady-state offset to remove. At rest on a level rail, zero force holds any position. Only a wind force on the payload leaves a sustained offset for the integral term to remove.

12.4.2 The Closed-Loop Sway Mode

Linearizing Equation (12.1) about $\theta = 0$, closing the position loop with gain K_c and velocity feedback $K_c\tau_D$, and retaining the drive lag gives a fifth-order system in $(x, \dot{x}, \theta, \dot{\theta}, F)$. Setting the drive lag aside for a moment, eliminating x between the two linearized balances gives the quartic of Equation (12.7).

$$\begin{aligned} M\ell s^4 + \big[(M+m)d + c\ell\big]s^3 + \big[(M+m)g + cd + K_c\ell\big]s^2 \\ + \big[cg + K_c d\big]s + K_c g = 0 \end{aligned} \tag{12.7}$$

where $c = b + K_c\tau_D$ is the total velocity feedback seen by the trolley and $d = 2\zeta\omega_n\ell$ is the pivot damping coefficient. Two of the four roots are the position loop and two are the sway mode. Three limiting cases bracket the sway root. A rigidly held trolley gives $\sqrt{g/\ell}$, or 4.012 s at 4 m. A completely free trolley gives the free-cart value $\sqrt{g(M+m)/(M\ell)}$, or 3.783 s, because the trolley recoils as the load swings and shortens the period. A trolley held by a finite spring lies between the two, and K_c decides where.

Restoring the drive lag turns the quartic into the fifth-order system of Equation (12.8) in the states $(x, \dot{x}, \theta, \dot{\theta}, F)$.

$$\begin{bmatrix} M+m & m\ell \\ 1 & \ell \end{bmatrix} \begin{bmatrix} \ddot{x} \\ \ddot{\theta} \end{bmatrix} = \begin{bmatrix} F - b\dot{x} \\ -g\theta - d\dot{\theta} \end{bmatrix}, \qquad \tau_a \dot{F} = -K_c x - K_c\tau_D \dot{x} - F \tag{12.8}$$

The control law has been linearized about a stationary setpoint with the integral term dropped, which is exact at $\tau_I = 1000$ s over the timescale of one swing, and the derivative filter is dropped as well because $\tau_f = 0.02$ s is two decades faster than anything else in the loop. Solving the eigenproblem at the default tuning gives a sway mode with a period of 3.8835 s and a damping ratio of 0.0579. The simulator, driven by the standard 6 m move with the shaper off and timed over thirteen zero crossings of the free decay that follows $t = 12$ s, returns 3.884 s and an amplitude decay time of 10.38 s against the predicted 10.65 s. The same calculation at 8 m predicts 5.5929 s and 15.22 s against a measured 5.5974 s and 15.02 s, and at 300 kg it predicts 3.7445 s and 6.10 s against a measured 3.743 s and 5.90 s.

Two consequences follow. The first is that the true sway frequency is 3.3 % above the $\sqrt{g/\ell}$ that the shaper formulas use, which is small but, as Section 12.4.4 shows, is not small compared with the tolerance of a two-impulse shaper. The second is that the closed position loop damps the payload. The sway damping ratio rises from the plant's 0.015 to 0.058, a factor of 3.9, because a swinging load pushes the trolley with a horizontal force of about $mg\theta$, the loop resists that push, and the drive dissipates the energy. The effect is incidental to the shaper and is the only mechanism the shaped loop has for removing sway that is already present.

12.4.3 Impulse Amplitudes and Times

Section 1.4.8 derives both shapers for an undamped mode. This section keeps the sway damping, which the formulas of this crane carry. An impulse of amplitude A_i applied at time t_i to a second-order mode of frequency ω and damping ratio ζ leaves, at any common time $t_n \geq \max_i t_i$, a sinusoidal residue whose vector magnitude is $A_i e^{-\zeta\omega(t_n - t_i)}$ and whose phase is $\omega_d t_i$. A sequence of impulses leaves the vector sum, so the residual vibration relative to what a single unit impulse would leave is Equation (12.9).

$$V(\omega,\zeta) = e^{-\zeta\omega t_n}\sqrt{C^2 + S^2}, \qquad C = \textstyle\sum_i A_i e^{\zeta\omega t_i}\cos(\omega_d t_i), \quad S = \sum_i A_i e^{\zeta\omega t_i}\sin(\omega_d t_i) \tag{12.9}$$

For two impulses at $t_1 = 0$ and $t_2 = \Delta$, setting $S = 0$ requires $\sin(\omega_d\Delta) = 0$, whose smallest positive solution is $\Delta = \pi/\omega_d$, one damped half period. Setting $C = 0$ then requires $A_1 = A_2 e^{\zeta\omega\Delta}$, and imposing $A_1 + A_2 = 1$ so that the shaped command reaches the same final value completes the zero-vibration shaper of Equation (12.10).

$$\mathbf{A}_{ZV} = \frac{1}{1+K}\begin{bmatrix} 1 \\ K \end{bmatrix}, \qquad \mathbf{t}_{ZV} = \begin{bmatrix} 0 \\ \pi/\omega_d \end{bmatrix} \tag{12.10}$$

where $K = \exp(-\zeta\pi/\sqrt{1-\zeta^2})$ is the factor by which the free response decays over one damped half period. Requiring in addition that $\partial V/\partial\omega = 0$ at the design frequency adds one constraint and

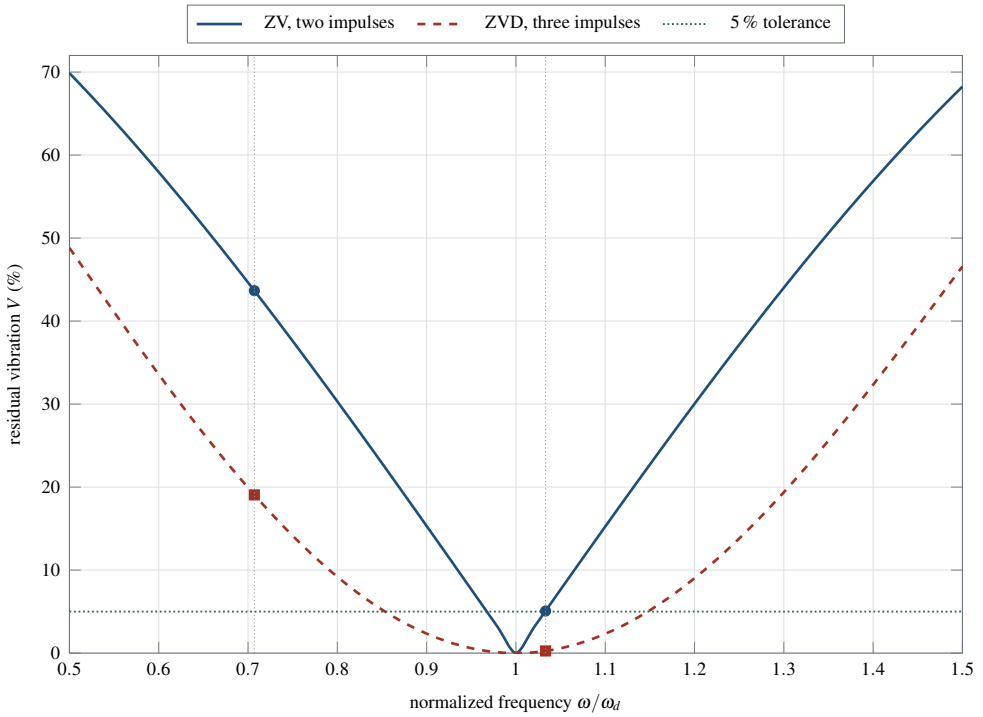


Figure 12.2 Residual vibration left by the two shapers as implemented, against plant frequency normalized to the design frequency, at $\zeta_a = 0.015$. Two impulses are solid with circles, three impulses dashed with squares, and the dotted horizontal is the 5 % tolerance. The dotted verticals are the two cases quantified in Section 12.6, the true coupled mode at $\omega/\omega_d = 1.0332$ when the shaper is given the nominal 4.00 m, and 0.707 for an 8 m cable with the shaper still set to 4 m.

therefore one impulse, and the solution is the zero-vibration-and-derivative shaper of Equation (12.11), which is the convolution of the two-impulse shaper with itself.

$$\mathbf{A}_{ZVD} = \frac{1}{(1+K)^2}\begin{bmatrix}1\\2K\\K^2\end{bmatrix}, \qquad \mathbf{t}_{ZVD} = \begin{bmatrix}0\\\pi/\omega_d\\2\pi/\omega_d\end{bmatrix} \tag{12.11}$$

The shaped command is the convolution of the raw setpoint history with the impulse train, as shown in Equation (12.12).

$$x_{SP}^{sh}(t) = \sum_i A_i\, x_{SP}(t - t_i), \qquad \sum_i A_i = 1 \tag{12.12}$$

Because the amplitudes sum to unity the trolley still arrives at the same place. It simply gets there one damped half period later for the two-impulse shaper and two for the three-impulse one, and that delay is the price of the cancellation rather than an implementation artifact. At the default $\zeta_a = 0.015$ and $\ell_a = 4.00\,\text{m}$ the impulse train is $[0.5118, 0.4882]$ at $[0, 2.006]$ seconds for the two-impulse shaper and $[0.2619, 0.4997, 0.2384]$ at $[0, 2.006, 4.013]$ seconds for the three-impulse one, because $K = 0.9540$. At an 8 m cable the half period grows to 2.837 s and the amplitudes do not change at all, because they depend only on ζ_a.

12.4.4 Residual Vibration Sensitivity

Evaluating Equation (12.9) with the impulse trains of Equations (12.10) and (12.11) held fixed at their design values while the plant frequency is swept produces the two curves of Figure 12.2. Both vanish at the design frequency. The two-impulse curve leaves it linearly and the three-impulse curve leaves it quadratically, which is the whole content of the extra derivative constraint. Holding the residual below 5 % of the unshaped value requires the plant frequency to lie within 0.968 to 1.033 of the design value for the two-impulse shaper, a total width of 0.065, and within 0.854 to 1.148 for the three-impulse one, a width of 0.294. Insensitivity improves by a factor of 4.5 for one extra damped half period of delay.

Two predictions follow immediately, and both are tested in Section 12.6. Entering the nominal 4.00 m into a shaper is not the best available choice, because the true coupled mode sits at 1.0332 of that design frequency, just outside the two-impulse tolerance band, where Figure 12.2 gives $V = 5.07\,\%$ against $V = 0.26\,\%$ for three impulses. The assumed length that puts the design frequency on the true mode is $\ell_a = g/\omega^2 = 3.75\,\mathrm{m}$, not 4.00 m. Doubling the cable to 8 m without retuning divides the plant frequency by $\sqrt{2}$, which lands at 0.707 where the curves give 43.7 % and 19.1 %. A two-impulse shaper at that frequency error removes 56 % of the residual the unshaped command would leave instead of all of it, and a three-impulse shaper removes 81 %.

12.5 Controller Design

12.5.1 The Discrete Algorithm

The whole control path runs to completion every $\Delta t_c = 0.01\,\mathrm{s}$ in both manual and automatic. The sequence is

1. push the current raw setpoint x_{SP} onto a delay line of 4096 samples stamped with the simulation time,
2. rebuild the impulse train from ℓ_a, ζ_a and g using Equation (12.10) or (12.11), or the single unit impulse at zero delay when the shaper is off,
3. form $x_{SP}^{sh} = \sum_i A_i\, x_{SP}(t - t_i)$ by sampling the delay line at each impulse time with linear interpolation,
4. evaluate F_{lim} from Equation (12.3) for the current payload mass and push the current tuning and limits into the loop,
5. in automatic, run the loop of Equations (12.14) and (12.15) on the error $e = x_{SP}^{sh} - x$ to get F_c,
6. in manual, form $F_c = \mathrm{clamp}(f_{man} + n_{key} F_{push}, \pm F_{lim})$ and call the loop in tracking mode against the same shaped reference,
7. slew limit the applied command, which gives $F_a \leftarrow \mathrm{slew}(F_c, F_a, \dot{F}_{max}, \Delta t_c)$,
8. raise the saturation flag when $|F_c| \geq F_{lim}$.

The delay line is seeded at $t = 0$ with the initial setpoint, and sampling before the oldest record returns that oldest value, so the pre-history the convolution assumes is genuinely constant and the first commanded step is shaped correctly. Because the initial setpoint is also the initial trolley position, the crane is in equilibrium while that pre-history is being written. Under the predictive controller of Section 12.5.4, step 5 takes F_c from the plan and the loop runs in tracking mode as in step 6.

12.5.2 Velocity Form Position Loop

The position loop computes an increment to the drive force each control interval rather than the force itself, which makes the algorithm the incremental, or velocity, form of the PID law [1, 18] of Section 1.6.2. The derivative acts on a filtered measurement rather than on the error, so a setpoint move produces no derivative kick. The error, the filtered position and the three increments are given by Equations (12.13) and (12.14).

$$e_k = x^{sh}_{SP,k} - x_k, \qquad \hat{x}_k = (1-a)\,x_k + a\,\hat{x}_{k-1} \tag{12.13}$$

$$\begin{aligned} \Delta u^P_k &= K_c\,(e_k - e_{k-1}) \\ \Delta u^I_k &= \frac{K_c}{\tau_I}\,e_k\,\Delta t_c \\ \Delta u^D_k &= -K_c\,\tau_D\left(\dot{\hat{x}}_k - \dot{\hat{x}}_{k-1}\right), \quad \dot{\hat{x}}_k = \frac{\hat{x}_k - \hat{x}_{k-1}}{\Delta t_c} \end{aligned} \tag{12.14}$$

where $a = e^{-\Delta t_c/\tau_f}$ is the exact zero-order-hold coefficient of the derivative filter, which is unconditionally stable at any ratio of step to time constant, and $\hat{x}$ is the filtered position the derivative estimate is taken from. The code forms each increment as the difference between the complete proportional or derivative term at two successive scans, which reduces to Equation (12.14) at constant gains and makes a gain change act at once. The increments are combined and the demand is passed through the force limit and the slew limit, as shown in Equation (12.15).

$$\begin{aligned} s_k &= s_{k-1} + \Delta u^P_k + \Delta u^D_k \\ c_k &= s_k + I_{k-1} \\ F_{c,k} &= \mathrm{slew}\big(\mathrm{clamp}(c_k, \pm F_{lim}),\, F_{c,k-1},\, \dot{F}_{max},\, \Delta t_c\big) \\ I_k &= I_{k-1} + \Delta u^I_k + \frac{\Delta t_c}{T_t}\left(F_{c,k} - c_k\right) \end{aligned} \tag{12.15}$$

Here s_k accumulates the proportional and derivative increments without limit (the S_k of Equation (1.13)), c_k is the force the algorithm demands (the v_k of Equation (1.14)), $F_{c,k}$ is that demand clamped to the force limit and slew limited, and I_k carries the integral contribution. The integral used at scan k was accumulated through scan $k-1$. Anti-windup is back-calculation with tracking time $T_t = \tau_I$, applied only when $K_I = K_c/\tau_I$ is nonzero, which holds at every τ_I the application offers. While the command is clipped, the last term drives I toward the value that reproduces the force actually emitted, so the integral term alone is corrected and the running sum s_k is never truncated [18]. Away from the limits the recursion is algebraically identical to the positional law with the same three gains, and Section 1.6.2 explains why the running sum is never clipped. At the default $\tau_I = 1000\,\mathrm{s}$ each scan removes only 10^{-5} of the clipped excess, which leaves the back-calculation nearly inert, but the integral it guards is equally small because $K_I = 0.62\,\mathrm{N/(m\,s)}$. In the saturated runs of Section 12.6 the integral term never exceeds 18.1 N, against force limits of 1200 N to 4000 N, so windup plays no part in any result reported here and the application offers no windup switch. The loop drives the trolley in the direction of a positive error, because more force moves the trolley in the $+x$ direction, and no action switch is offered. Three limits act in series on the way to the plant, the clamp and the slew limit inside Equation (12.15) and the slew limit applied again to F_a, after which the first-order drive of Equation (12.3) rounds off whatever is left. The effective actuator is therefore slower than any one of those three numbers suggests, and a 6 m move that commands a peak of 3428 N develops a peak of 3046 N.

No coefficient in Equation (12.14) changes when the shaper is switched on. The shaper writes x^{sh}_{SP} and nothing else, which is why the comparison between a shaped and an unshaped run in Section 12.6 is a controlled experiment with exactly one difference in it.

12.5.3 Transfer and Manual Operation

Transfer is bumpless in both directions, as in every framework app (Section 1.6.2). In manual the loop runs in tracking mode against the shaped reference, which sets I_k so that c_k equals the operator's own force, and in automatic the controller output is copied to the manual input after every scan.

The manual station puts the size of the problem in front of the operator before any theory is offered. The drive force is entered directly over $\pm 4000\,\mathrm{N}$, held at $\pm 2400\,\mathrm{N}$ for as long as an incremental command is applied, or delivered as a fixed 0.8 s push of the same size. Driving a 6 m move by hand and stopping the trolley on the target is straightforward. Stopping the load with it is not, which is the first demonstration that the second half of the task is a timing problem rather than a force problem.

12.5.4 Model Predictive Control on the Shaper's Model

A model predictive controller (MPC), selected only by configuration 12, decides the drive force rather than the reference. Each plan covers the next $T_p = 6\,\mathrm{s}$, only its start is applied, and a new plan follows (Section 1.6.3), the receding-horizon law whose constrained form and terminal costs are reviewed in [19], whose industrial use is surveyed in [20], and which has bounded the swing of a laboratory crane [21].

The controller's model is not identified. It is Equation (12.1) linearized at a vertical cable without the centripetal term, completed by the drive lag, a ramped command and a constant horizontal force w on the payload, as shown in Equation (12.16).

$$\begin{bmatrix} M_0 + m_0 & m_0 \ell_a \\ 1 & \ell_a \end{bmatrix} \begin{bmatrix} \ddot{x} \\ \ddot{\theta} \end{bmatrix} = \begin{bmatrix} F + w - b_0 \dot{x} \\ -g\theta - d_a \dot{\theta} + w/m_0 \end{bmatrix}, \qquad \tau_{a0} \dot{F} = F_c - F, \qquad \dot{F}_c = \rho, \qquad \dot{w} = 0 \tag{12.16}$$

Here ρ is the force rate the controller decides, $d_a = 2\zeta_a \omega_a \ell_a$ with $\omega_a = \sqrt{g/\ell_a}$, and the subscript 0 marks a declared value of Table 12.2. The cable length, damping ratio and gravity are the shaper's, so a wrong cable length misleads both controllers alike, while the masses, rail damping and drive lag stay declared whatever the plant does. Driven open loop by the shaped loop's force, the model follows the simulated swing to 0.002° over 15 s of configuration 3 but errs by 18.0° on the 8 m cable with the model at 4 m.

A zero-order hold over the decision period $T_s = 50\,\mathrm{ms}$, every fifth control interval, gives steps k up to $N = T_p/T_s = 120$. The decisions are force rates over six move blocks of 1, 2, 4, 8, 16 and 89 steps, so the planned command is piecewise linear, which the slew limit passes unchanged, and between decisions F_c follows the first planned ramp. The objective is Equation (12.17).

$$J = \sum_{k=1}^{N-1} \left\| S^{-1}(y_k - y^*) \right\|^2 + \lambda \sum_{k=0}^{N-1} \frac{\rho_k^2}{s_\rho^2} + \tilde{z}_N^T P \tilde{z}_N + \sum_{i \in \{\theta, x\}} \left(q_i \varepsilon_i^2 + r_i \varepsilon_i \right) \tag{12.17}$$

Here $y = (x + \ell_a\theta,\, \dot{x},\, \theta,\, \dot{\theta}/\omega_a,\, F_c)$ and $y^* = (x_{SP} + \ell_a\theta_{ss},\, 0,\, \theta_{ss},\, 0,\, F_{ss})$ is rest at the setpoint with $\theta_{ss} = \hat{w}/(m_0 g)$ and $F_{ss} = -\hat{w}$, where $\hat{w}$ is the estimate of w. The scales are

$$S = \mathrm{diag}(0.6\,\mathrm{m},\, 0.6\,\mathrm{m/s},\, 6^\circ,\, 6^\circ,\, 4000\,\mathrm{N})$$

with $s_\rho = 12\,\mathrm{kN/s}$ and $\lambda = 300$, chosen once on configuration 12 as the least force travel among the 265 of 1008 settings of the first three scales and λ within 10 % of the shortest time to a quiet payload, all of which kept the swing at or below the 3.23° of three impulses. $\tilde{z}_N$ is the departure of the first six states from rest, and P solves the discrete Riccati equation for the same weights, the cost-to-go of the linear quadratic regulator (LQR). With every step free and no limit binding, the first planned rate is the LQR's to $2.3 \times 10^{-5}\,\mathrm{N/s}$ on moves of up to 339 N/s.

Table 12.3 The Thirteen Shipped Configurations and Their Subjects

Configuration	What it changes and what it shows
1 Fast move	6 m, shaper off. The residual sway a good position loop leaves behind.
2 Two impulses	Same move, same gains, shaped reference.
3 Three impulses	One more half period of delay against the 3.3 % nominal frequency error.
4 Long cable	Hoist +4 m. The $\sqrt{2}$ scaling of Equation (12.4), and a retuned shaper.
5 Wrong length	8 m cable, shaper still told 4 m. Figure 12.2 at 0.707.
6 Heavy payload	300 kg. Mass detunes the loop, length detunes the shaper.
7 Force saturation	10 m move on a 1200 N drive. Feedforward against a pinned actuator.
8 Derated drive	1400 N. Slowing the crane down as the operator's own anti-sway method.
9 Already swinging	$\theta_0 = 8°$, no move commanded. A shaper with nothing to shape.
10 Repeated moves	Four moves at 1.5, 14, 28 and 42 s including a 0.5 m trim. Convolution and overlap.
11 Wind	120 N on the payload with $\tau_l = 10$ s. A load disturbance, not a command.
12 Shaper against MPC	The move of 1 to 3 under the predictive controller, the loop preset to three impulses. Prediction against cancellation.
13 Challenge	8 m move from a deliberately poor tuning against three simultaneous targets.

The limits $|\rho_k| \le \dot{F}_{max}$ and $|F_c| \le F_{lim}$, the latter at every block end and so everywhere, are hard and read where the position loop reads them. The slacks $\varepsilon_i \ge 0$ soften two limits judged every 0.1 s of the plan, $|\theta_k - \theta_{ss}| \le \theta_{max}$ with $\theta_{max} = 3°$, $q_\theta = 10^8$ per rad^2 and $r_\theta = 10^6$ per radian, and $0 \le x_k \le x_{max}$ with $x_{max} = 24$ m, $q_x = 10^4$ per m^2 and $r_x = 10^3$ per meter, because a hard state limit can be infeasible. Each plan is a quadratic program in eight variables with 266 inequality rows and a ridge of 5.0×10^{-7}, solved in 2.9 dual active-set iterations on average.

A steady-state Kalman filter on $(x, \dot{x}, \theta, \dot{\theta}, F, w)$ at Δt_c, driven by the applied force, supplies the initial state from the trolley position, and from the swing angle as well when the optional sensor is on, with measurement variances $(1\,\text{mm})^2$ and $(0.05°)^2$ and process variances of 10^{-9}, 10^{-6}, 10^{-12}, 10^{-6}, 1 and 1 per interval in SI units. The swing reaches the position only through the recoil $m_0 g\theta/M_0$, 0.0214 m/s^2 per degree or 7.67 mm of free trolley motion per degree of swing, which leaves the filter observable at a condition number of 9.5×10^4, and its estimate stays within 0.038° of the swing in configuration 12. The state w is the integrating disturbance that makes the MPC offset free [22], as the fuel bias does for the boiler of Volume 9, Chapter 4.

A plan that is not optimal, whose first rate is not finite or exceeds $\dot{F}_{max}$, or whose first block ends beyond F_{lim} is rejected. The position loop, which tracks the applied force while the MPC drives, then takes the drive until the next accepted plan. Three rejections forced at seven instants of configuration 12 move the command by at most 12.4 N, against steps of up to 34.9 N between scans of the undisturbed run, and no shipped configuration rejects any of its 600 plans in 30 s. The plant itself remains the nonlinear Equations (12.1) to (12.3) at the true values, read through the exact position and, optionally, the exact angle. A plan takes 211 µs on average in Node.js and 0.3 to 0.6 ms in Chrome, at most 1.2 % of a core at real time.

12.6 Results

The thirteen configurations shipped with the application are named in Table 12.3 beside the mechanism each is built around. A configuration fixes only the disturbance, drive rating, shaper or tuning its own subject requires and inherits every other value from Table 12.2, which keeps the single change under examination identifiable. Every configuration except 9 commands its first move as a timed setpoint step at $t = 1.5$ s, after which the crane is at rest at a new target and the run continues until the payload has quieted or has demonstrated that it will not.

Table 12.4 collects the outcome of every configuration and of the variants discussed below. All values come from the running application over a common 30 s horizon, with every setting changed before the run starts. The parking time is the first logged instant after which the trolley stays inside

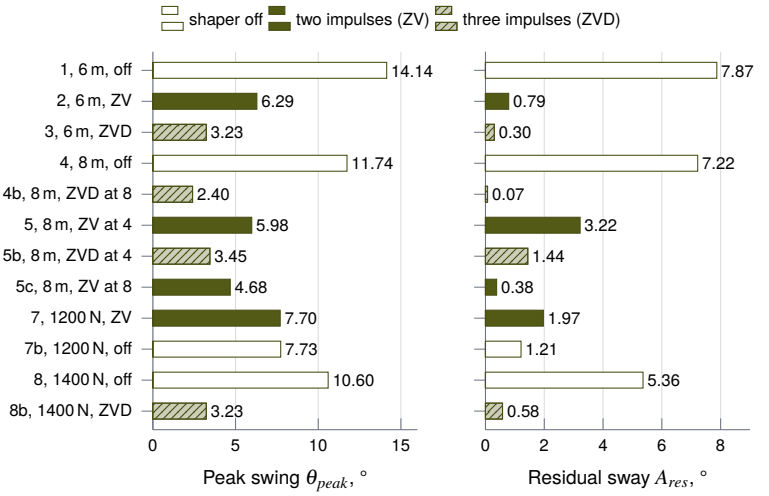


Figure 12.3 Peak swing and residual sway at parking from Table 12.4: the standard move (rows 1 to 3), the 8 m cable with the shaper told 4 or 8 m (rows 4 to 5c), the 1200 N drive on a 10 m move (rows 7 and 7b) and the 1400 N drive (rows 8 and 8b). White bars have the shaper off, solid bars two impulses and hatched bars three. Notice that a shaper told the true cable length leaves a fraction of a degree, a mistuned one leaves several times more, and on the 1200 N drive the shaped and unshaped peaks are the same.

± 0.10 m of the *raw* target for the rest of the run, A_{res} is the sway amplitude of Equation (12.5) at that instant, and A_{20} is the same amplitude at the fixed time $t = 20$ s, where the window over which the graded challenge is scored begins. All three are read from the 50 Hz record the application exports. The peak swing angle and the force-limited percentage are the application's own figures, the first updated at every 5 ms integration step, and the peak commanded force is taken over every controller scan. Figure 12.3 draws the peak swing and the residual sway of the main rows.

> **+ DID YOU KNOW? A Weaker Drive Swings the Load Less**
>
> From the simulator: derating the drive from 4000 N to 1400 N, with no control change at all, lowers the residual sway of the standard move from 7.87° to 5.36°, because the trolley can no longer accelerate as hard. Three impulses on the same derated drive leave 0.58° (Table 12.4, rows 1, 8 and 8b).

12.6.1 Shaping on the Nominal Crane

Configurations 1, 2 and 3 differ in one setting. The unshaped move peaks at 14.14° of swing, parks at 9.88 s and leaves 7.87° behind, and the payload is still moving 2.81° at $t = 20$ s. The two-impulse shaper cuts the peak to 6.29° and the residual to 0.79°, a factor of 10.0 on the residual, and the three-impulse shaper reaches 3.23° and 0.30°, a further factor of 2.7. The gains are identical in all three runs.

Table 12.4 Measured Outcome of Every Configuration Over a 30 s Horizon

Configuration	t_{park} (s)	θ_{peak} (deg)	A_{res} (deg)	A_{20} (deg)	$\lvert F_c \rvert_{peak}$ (N)	sat (%)
1 Fast move, off	9.88	14.14	7.87	2.81	3428	0.0
2 Two impulses	11.54	6.29	0.79	0.26	1935	0.0
3 Three impulses	12.72	3.23	0.30	0.07	1894	0.0
4 8 m, off	11.64	11.74	7.22	4.10	3428	0.0
4b 8 m, ZVD at 8	14.04	2.40	0.07	0.08	1828	0.0
5 8 m, ZV at 4	12.24	5.98	3.22	1.95	1914	0.0
5b 8 m, ZVD at 4	13.06	3.45	1.44	0.94	1882	0.0
5c 8 m, ZV at 8	12.14	4.68	0.38	0.32	1851	0.0
6 300 kg, ZV	11.14	6.00	0.96	0.15	2037	0.0
6b 300 kg, off	9.54	12.02	5.05	0.75	3429	0.0
7 1200 N, ZV	12.90	7.70	1.97	0.87	1200	10.1
7b 1200 N, off	12.86	7.73	1.21	0.49	1200	11.5
7c $K_c = 60$, off	26.32	3.56	0.70	—	600	0.0
7d $K_c = 60$, ZV	27.50	1.82	0.11	—	540	0.0
8 1400 N, off	10.40	10.60	5.36	2.12	1400	4.8
8b 1400 N, ZVD	12.74	3.23	0.58	0.22	1400	1.2
9 Already swinging, ZVD	—	8.02	—	1.29	124	0.0
11 Wind, ZVD, $\tau_I = 10$	—	8.18	—	4.28	1828	0.0
12 MPC	9.68	3.00	1.10	0.00	1043	0.0
13 Challenge, as loaded	26.10	13.29	2.95	4.32	2388	0.0
13b Challenge, tuned	14.32	4.26	0.15	0.16	2587	0.0
13c Challenge gains, off	12.88	18.55	7.59	3.85	4000	0.5

Rows 1 to 6, 8 and 12 are the standard 6 m move, rows 7 are 10 m and rows 13 are 8 m. Rows 6 and 7 are the configurations as shipped, with the two-impulse shaper on, and rows 6b and 7b switch it off. $\lvert F_c \rvert_{peak}$ is the peak commanded force, which the drive lag and the two slew limits reduce before it reaches the trolley. An em dash means the quantity does not apply, because the trolley never leaves its target in row 9, never settles inside the band in row 11, and has not yet parked at 20 s in rows 7c and 7d. Configuration 10 is discussed in the text rather than tabulated, because a sequence of four moves has no single parking time.

> **TRY IT IN THE APP** **2 · ZV Input Shaping**
>
> Load the scenario, press Run and watch the dashed shaped setpoint on the position trend. It climbs in two steps 2.006 s apart, and the swing the first step starts is canceled by the second. The peak sway reads 6.29° and the residual 0.79°, against 14.14° and 7.87° with the shaper off.

Two side effects are visible in the same table. The parking time grows from 9.88 s to 11.54 s and 12.72 s, which is 1.66 s and 2.84 s against shaper spans of 2.006 s and 4.013 s, the difference being that the loop was never going to track the raw step instantly either. The peak commanded force falls from 3428 N to 1935 N and 1894 N, because the loop is never presented with the whole 6 m error at once. Shaping buys actuator headroom as a side effect, and configuration 13 turns that side effect into the difference between passing and failing.

The three-impulse advantage on a crane that is not obviously mistuned is exactly the 3.3 % frequency error of Section 12.4. Figure 12.2 predicts 5.07 % residual for two impulses at that point and 0.26 % for three, a ratio of 20. The measured ratio of residuals is 2.7, which is far smaller, and the difference follows from the assumptions behind the prediction. Equation (12.9) describes a mode driven directly by the shaped signal through a linear time-invariant path. Here the mode is driven by the trolley acceleration produced by a saturating, slew-limited, lagged and trigonometrically nonlinear

closed loop, which puts a floor under the achievable residual. A sweep of the assumed length through $\ell_a = 2.5\,\text{m}$ to $8.0\,\text{m}$ locates that floor. The best A_{20} a two-impulse shaper reaches anywhere in the sweep is $0.210°$ and the best a three-impulse shaper reaches is $0.047°$, against $2.81°$ unshaped, so neither is reaching the zero that Equation (12.9) promises.

What the sweep does confirm is the position and the width of the two minima. The two-impulse residual is smallest at $\ell_a = 3.75\,\text{m}$, which is the value g/ω^2 predicted from the closed-loop mode of Section 12.4 and one grid step below the nominal $4.00\,\text{m}$, and it rises to $0.810°$ at $\ell_a = 5.0\,\text{m}$ and $2.138°$ at $\ell_a = 8.0\,\text{m}$. The three-impulse residual stays below $0.180°$ across the whole range $\ell_a = 3.0\,\text{m}$ to $5.0\,\text{m}$, where the two-impulse residual varies by a factor of 3.8.

12.6.2 Effect of Cable Length and Payload Mass

Paying out four meters of cable doubles ℓ and, by Equation (12.4), divides the frequency by $\sqrt{2}$. The predicted period rises from $4.012\,\text{s}$ to $5.674\,\text{s}$ and the measured closed-loop mode from $3.884\,\text{s}$ to $5.597\,\text{s}$, a measured ratio of 1.441 against the predicted 1.414. The payload mass does not appear in Equation (12.4) at all, and doubling it to $300\,\text{kg}$ moves the measured period only from $3.884\,\text{s}$ to $3.743\,\text{s}$, a shift of $3.6\,\%$ that comes entirely from the trolley recoiling harder against a heavier load. The two-impulse shaper survives that untouched, with the residual moving from $0.79°$ to $0.96°$ against $5.05°$ for the same move with no shaping.

The mistuned case is the sharpest test in the set. With a true $8\,\text{m}$ cable and a shaper still told $4\,\text{m}$, the second impulse lands $2.006\,\text{s}$ after the first when the payload needs $2.837\,\text{s}$, and the normalized frequency is 0.707. Four residuals on the same move quantify the loss. Doing nothing leaves $7.22°$, the mistuned two-impulse shaper leaves $3.22°$, the mistuned three-impulse shaper leaves $1.44°$, and a correctly tuned two-impulse shaper leaves $0.38°$. Expressed as fractions of the unshaped residual, the two mistuned shapers leave $44.6\,\%$ and $19.9\,\%$, against the $43.7\,\%$ and $19.1\,\%$ that Figure 12.2 predicts from Equation (12.9) alone. The sensitivity curve is quantitatively accurate where the frequency error is large, to within $5\,\%$ of the measured fractions. Retuning the three-impulse shaper to the true $8\,\text{m}$ recovers everything and more, at $2.40°$ of peak and $0.07°$ of residual.

The industrial literature reaches the same conclusion [12]. Robustness is not a substitute for knowing the cable length. It is insurance against the error that remains after the length has been measured as well as it can be, which is why a production system computes the impulse train from a live drum encoder and why the assumed length is a separate control in this application rather than being wired to the truth.

12.6.3 Conditions Under Which Shaping Fails

Three configurations show the method failing, and none of the three is repaired by retuning.

A $10\,\text{m}$ command at $K_c = 620\,\text{N/m}$ asks for $6200\,\text{N}$ from a drive rated at $1200\,\text{N}$. Shaping on and shaping off then give the same peak sway to within $0.4\,\%$, $7.70°$ against $7.73°$, and the shaped run ends with *more* residual sway, $1.97°$ against $1.21°$. The drive spends $10.1\,\%$ and $11.5\,\%$ of the run pinned at its limit, and while it is pinned the trolley is following the force limit rather than the reference, so reshaping the reference changes nothing that reaches the payload. Dropping the gain to $K_c = 60\,\text{N/m}$ keeps the peak command at $600\,\text{N}$, well inside the limit, and shaping immediately works again, cutting the peak from $3.56°$ to $1.82°$ and the residual from $0.70°$ to $0.11°$. Input shaping is a statement about a linear system, because convolution commutes with linear time-invariant dynamics and with nothing else. An actuator on its limit is not following the input at all, and a better shaper does not repair that. Making the commanded move something the actuator can execute does.

🕮 **Pause.** Try Exercise 12.3 before reading on.

> **TRY IT IN THE APP 7 · Drive Force Saturation**
>
> Run the scenario and watch the drive force sit on its 1200 N limit. The peak sway is 7.70° with two impulses and 7.73° without them, and the shaped run ends with more residual sway. Reload, set Proportional gain to 60 N/m and run again: the shaper now cuts the peak from 3.56° to 1.82°.

Starting the payload at 8° with no move commanded is the complementary failure. The three-impulse shaper is enabled and has no effect, because the setpoint never changes and a convolution with a constant returns that constant. Command shaping prevents sway that a command would otherwise have caused and has no mechanism whatever for removing sway that is already present. What does remove it is the position loop, through the accidental damping quantified in Section 12.4. The swing falls from 8.02° to 1.29° in 20 s, a log-linear fit over the decay giving an amplitude decay time of 10.4 s against the 42.6 s the cable pivot would give on its own, and the largest force the loop ever commands while doing it is 124 N.

Pause. Try Exercise 12.1 before reading on.

A steady 120 N wind on the payload is the third case, and it separates two mechanisms that are easy to confuse. At steady state the cable must tilt until its horizontal component balances the wind, so $\tan\theta = W/(mg)$ and the payload hangs at $\arctan(120/(150\times 9.81)) = 4.662°$ for as long as the wind blows. The application settles at 4.662°. No shaper and no position tuning can touch that, because the loop cannot reach θ. The trolley is a different matter. Holding station against the wind needs a steady 120 N of drive force, and proportional action alone can only produce it by sitting $W/K_c = 120/620 = 0.194$ m off target. Running the same case at the default $\tau_I = 1000$ s, which is slow enough to contribute almost nothing over a move, leaves the trolley 0.200 m past a 6.000 m target at 60 s with the drive holding −120.1 N, and the small excess over 0.194 m is integral action the loop has not yet unwound. The two problems have different mechanisms and neither remedy substitutes for the other.

12.6.4 Derated Drive, Repeated Moves and the Graded Challenge

Derating the drive from 4000 N to 1400 N lowers the peak sway from 14.14° to 10.60° and the residual from 7.87° to 5.36° with no control change at all, because sway is driven by trolley acceleration and the trolley can no longer accelerate as hard. That is the anti-sway method operators apply by hand, and it is the expensive one, because the reduction is paid for in move time on every cycle. The three-impulse shaper on the same derated drive gives 3.23° of peak and 0.58° of residual for one extra half period, and the 0.58° is worse than the 0.30° of the full-power case because the drive still spends 0.36 s on its limit, 1.2 % of the 30 s run, against 1.45 s with the shaper off.

Four moves in sequence show that the convolution is indifferent to the complexity of the setpoint history. Reading the sway amplitude at the last logged sample before the second, third and fourth commands and at the end of the 56 s run, the shaped run is at 0.013, 0.191, 0.273 and 0.061° while the unshaped run is at 4.25, 5.61, 7.21 and 2.17°. Peak sway over the whole sequence is 4.27° shaped and 21.75° unshaped. The shaper handles a 0.5 m trim and a 7 m traverse with the same relative treatment, and it handles a move that starts before the previous one has settled, because none of that is visible to a linear convolution. What accumulates in the unshaped run is sway from each move adding to the sway still left from the last one, which is what makes an unshaped crane demanding to drive.

The graded challenge asks for an 8 m move that holds the trolley within ±0.10 m of the target and the sway amplitude below 1.0° from $t = 20$ s to the end of a 30 s run, with no time at all on the force limit, starting from $K_c = 300$ N/m, $\tau_D = 0.5$ s and the shaper off. As loaded it fails the first two targets, overshooting to 9.90 m and not parking until 26.10 s, so the worst position error after 20 s is 0.14 m and the sway amplitude is still 4.32°. The order in which the three changes are made is what the challenge teaches. Raising τ_D to 2.5 s cuts the overshoot from 24 % to 0.8 %, because derivative action is the only damping Equation (12.6) offers, and raising K_c to 660 N/m makes the

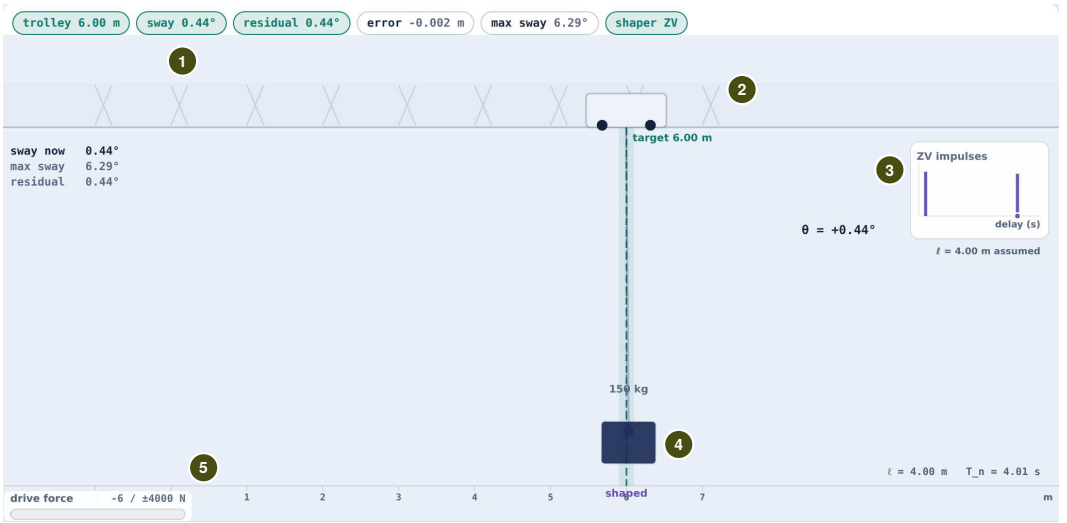


Figure 12.4 The two-impulse shaper on the standard 6 m move, paused at $t = 15$ s, cropped to the plant view. (1) The badges give the swing now, 0.44°, and its peak during the move. (2) The trolley stands at its target. (3) The impulse inset shows the two impulses of the shaped command, 0.512 and 0.488 separated by 2.006 s (Equation (12.10)), at the assumed cable length. (4) The load hangs nearly still above the shaped setpoint marker, leaving 0.44° against the 14.14° peak of the same move with the shaper switched off (Table 12.4). (5) The drive force is back near zero. The controller gains are unchanged.

move quick. Those gains alone, with the shaper still off, give 18.55° of peak sway, 7.59° of residual and a drive pinned at 4000 N for 0.16 s, 0.5 % of the run, so the sway and saturation targets are still missed although the trolley parks. Adding the three-impulse shaper makes the first commanded step $8 \times 0.262 = 2.10$ m instead of 8 m, which drops the peak command to 2587 N and takes the drive off its limit entirely, and the run parks at 14.32 s with 4.26° of peak sway and 0.15° of residual. Over the scored window the worst position error is then 0.02 m and the largest sway amplitude 0.16°, inside the targets by 0.08 m and 0.84°. Shaping returns nothing on a poorly damped loop or on a saturated one, so it is added last rather than first.

12.6.5 Shaper Against Predictive Control

Table 12.5 sets the shaped loop at its shipped tuning beside the MPC at configuration 12's settings, in 30 s runs with one exact trolley position, one cable length and no preview for both. The quiet time t_{quiet} is the first instant after which the trolley stays parked and the swing amplitude at or below θ_{ok}.

On the standard move the MPC parks at 9.68 s and is quiet at 10.56 s, where three impulses do both at 12.72 s, with a peak swing at its own 3.00° limit against 3.23° and 55 % of the peak command, 1043 N against 1894 N. It parks with 1.10° on the load against 0.30° and removes that inside the band within 0.88 s. The shaper's command is three pulses of 963, 1883 and 955 N whose swings cancel, while the plan pushes in two lobes of 1016 and 1042 N and holds the swing on its limit for 1.44 s, as shown in Figure 12.5. Holding the trolley back meanwhile costs position IAE against two impulses, 25.61 m s against 23.94 m s, although three impulses reach 29.67 m s.

On the 8 m cable with both controllers told 4 m, the MPC is quiet at 18.70 s against 29.28 s for three impulses, and two impulses not within the run, but it loses on peak swing, 4.44° against 3.45°. Its estimate, inferred from the recoil through a 4 m pendulum, errs by up to 1.39°, about the 1.44° by which it passes its limit, and its prediction is that of the shorter cable. The sensor removes the first

Table 12.5 Shaped Loop Against MPC Given One Cable Length, Runs of 30 s

Case	Law	t_{park} (s)	t_{quiet} (s)	A_{res} (deg)	θ_{peak} (deg)	$\lvert F_c\rvert_{peak}$ (N)	Travel (N)	t_{lim} (s)
6 m	ZV	11.54	12.58	0.79	6.29	1935	6491	0
	ZVD	12.72	12.72	0.30	3.23	1894	6366	0
	MPC	9.68	10.56	1.10	3.00	1043	4101	0
8 m, at 4	ZVD	13.06	29.28	1.44	3.45	1882	6691	0
	MPC	10.64	18.70	1.49	4.44	1019	4995	0
	MPC+s	10.64	15.92	1.37	3.74	1027	3962	0
8 m, at 8	ZVD	14.04	14.04	0.07	2.40	1828	6427	0
	MPC	10.26	11.04	1.09	3.00	1315	4841	0
300 kg	ZV	11.14	12.48	0.96	6.00	2037	6686	0
	MPC	13.54	13.90	0.72	3.31	1111	9169	0
1200 N	ZV	12.90	25.48	1.97	7.70	1200	3996	3.04
	MPC	11.56	12.38	1.22	3.00	1200	5009	0.05
8° start	ZVD	—	29.86	—	8.02	124	1491	0
	MPC	6.44	10.34	1.61	8.02	522	2959	0

The rows are configurations 2, 3 and 12, then 5 and 4 on the 8 m cable with $\ell_a = 4$ m, 4 with $\ell_a = 8$ m, then 6, 7 and 9. ZV and ZVD are the shaped loop with two and three impulses, MPC+s the MPC with the sway sensor, Travel the summed change of the commanded force and t_{lim} the time on the force limit. Every MPC run makes 600 plans and rejects none.

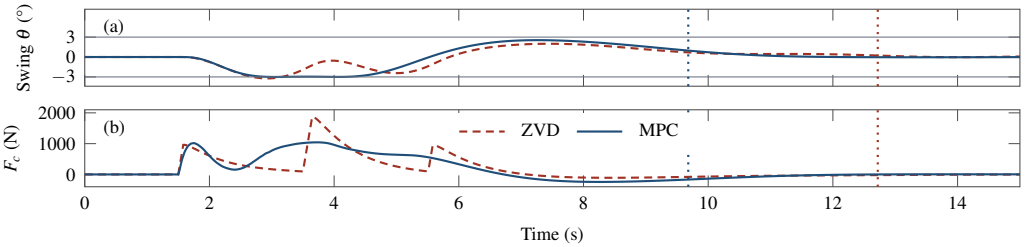


Figure 12.5 Configuration 12 from 0 to 15 s under the MPC and under the shaped loop with three impulses, both given the 4 m cable, the 6 m move commanded at 1.5 s. The MPC is solid and three impulses are dashed. (a) Swing angle against the ±3° limit of the plan (thin gray lines). (b) Commanded force. Dotted lines mark the parking instants, 9.68 s and 12.72 s.

error and not the second. It cuts the estimate error from 1.39° to 0.041° but the peak swing only from 4.44° to 3.74°. The 18.70 s belongs to the shipped settings. Over 20 combinations of decision period, block set and horizon the quiet time ranges from 14.3 to 25.4 s, while the peak stays between 3.9° and 5.4°, above the shaper's in every one. Told 8 m, both work, and the MPC is quiet 3.0 s sooner.

The MPC loses the doubled payload outright to two impulses, quiet at 13.90 s against 12.48 s with 9169 N of force travel against 6686 N, although it peaks at 3.31° against 6.00°. The recoil is twice what the model expects, w absorbs only part of it, and the estimate errs by 2.14°, while the shaper needs only a frequency that the mass moves by 3.6 %.

On the 1200 N drive the MPC rides the force limit, binding in 46 of its 600 plans, and is quiet at 12.38 s against 25.48 s. On the 1400 N drive its 1043 N peak never reaches the limit. The 8° initial swing, above 0.5° until 29.86 s under the shaped loop, is quiet at 10.34 s from the trolley position alone and at 8.28 s with the sensor, which then spends 0.15 s on the 4000 N limit. In the 120 N wind the estimate of w reaches 120.0 N and the trolley sits at 6.000 m at 30 s, where the loop with $\tau_I = 10$ s is at 6.133 m. With only the controller changed, the MPC meets all three targets of the challenge, parked at 10.64 s with 1.22° on the load, quiet from 11.48 s and never on the limit. The challenge is left as shipped, with the shaped loop's commissioning sequence as its suggested answer.

12.6.6 The Running Application

The application as it runs is reproduced in Figure 12.4. Its manual and automatic operation, scenarios and data export are those of every framework app (Section 1.6.4).

12.7 Technology in Practice

What Measures It

The shaped loop of this chapter needs one measurement, the trolley position, and one number entered by hand, the assumed cable length. On ship-to-shore cranes the second is measured too, by encoders on the hoisting rope, and the payload mass by weighing cells [4]. Those two readings are what a shaper needs in order to follow the hoist instead of waiting to be retuned, which is the gain scheduling that Section 12.6 performs by hand when it retells the shaper the true 8 m. The swing itself is not read by the shaped loop at all. The predictive controller's optional sensor stands for the cameras, lasers, inclinometers and inertial units that closed anti-sway loops use [23].

> **TECHNOLOGY Sensor: Rope Length, Load Mass and the Swing**
>
> On ship-to-shore cranes the length of the hoisting rope is read by digital encoders and the payload mass by weighing cells, both to about 5 %, so the rope length is known before a move [4]. A closed anti-sway loop needs further sensors for the load itself. Cameras with image processing, lasers, inclinometers and inertial units on the hook have all been used, and the inertial unit on the hook is small, cheap and need not be moved when the load changes [23]. The chapter's shaped loop reads the trolley position alone, and its assumed cable length is entered by hand.

What Moves It

A trolley drive is an electric motor fed by a frequency inverter, set by the operator's joystick as a desired trolley velocity on a quay crane, and on such a crane the motor pulls the trolley through gears, a drum and rope [4]. The drive's own torque and acceleration limits [24] are what the chapter models as F_{max} and $\dot{F}_{max}$, with a 0.08 s lag for the rest of its response. Those limits matter to the method, because a shaper is a linear device and the trolley leaves the linear range the moment the drive reaches its rating.

> **TECHNOLOGY Final Element: An Inverter-Fed Travel Drive**
>
> On a quay crane studied for anti-sway, the operator's joystick sets a desired trolley velocity, a frequency inverter controls the motors, and the motors wind or unwind rope on a drum through gears to pull the trolley [4]. Such drives limit speed, current and torque and the rate at which speed may change, and a host programmable logic controller can rewrite these limits while the motor runs [24]. The chapter's drive is a force source with a 4000 N rating, a slew limit and a first-order lag.

Where the Controller Runs

Programmable logic controllers serve as the primary controller of smaller systems that control discrete processes, and as local controllers under a supervisor in larger ones [25]. The chapter's controller runs every 0.01 s, the rate it names for a crane drive programmable logic controller. Its structure is a delay line of setpoints and an impulse train in front of a velocity-form PID block, followed by the clamp and the slew limits, and in a real installation the drive's own limits follow as well. Figure 12.6 draws the loop on that hardware.

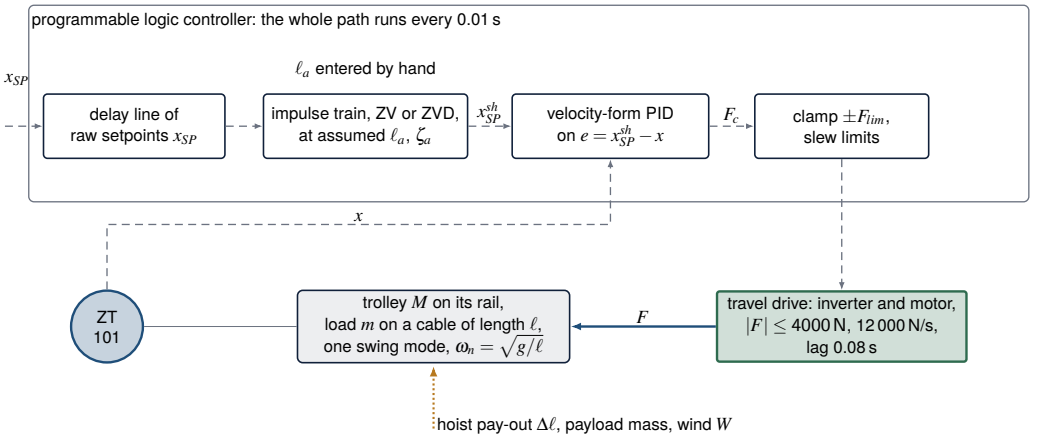


Figure 12.6 The crane loop on drive hardware. The trolley position ZT-101 is the only measurement. The raw setpoint passes a delay line and an impulse train evaluated at an assumed cable length entered by hand, the velocity-form PID acts on the shaped error, and the clamp and slew limits pass the command to the travel drive, which pushes the trolley. Hoisting, a change of payload and wind act on the crane. Notice that no path leads from the swing back to the drive, and that the impulse train learns of a hoisting change only if someone retells it the cable length.

> **IN PRACTICE** **What the Crane Rule Asks of the Operator**
>
> The United States rule for overhead and gantry cranes, 29 CFR 1910.179, requires that the hook be brought over the load so as to prevent swinging, that there be no sudden acceleration or deceleration of the moving load, and that the operator avoid carrying loads over people. Stops must be fitted at the limits of trolley travel, and bumpers must stop the crane at an average deceleration no greater than 3 ft/s^2 when it travels at 20 % of its rated load speed [26]. A shaped command is one way to move without the sudden acceleration the rule forbids.

What Is Modernizing It

Two developments are moving crane control beyond a fixed shaper. An inertial unit on the hook closed an anti-sway feedback loop on a five-ton industrial overhead crane and damped the first swing mode while the setpoint stood at zero, at the cost of slower tracking of the trolley velocity setpoint [23]. Image processing that tracks the payload has been used to measure how human operators drive an input-shaped bridge crane, and they finished obstacle courses faster and more safely with shaping on [17]. The predictive controller of Section 12.5.4 is a third path, and Section 12.6.5 measures what it gains and loses against the shapers when both are given the same cable length.

12.8 Limitations

The largest limitation is the single-mode payload. A real hook block on a sling is a double pendulum whose second mode is faster and lightly damped, and a shaper designed for one frequency leaves that mode untouched. Designing for two frequencies at once costs further delay and the trade has been worked out for tower and bridge cranes, but nothing in this application exhibits it.

The cable length is constant during every move. That assumption is the first to break in service, because cranes hoist and traverse together and the frequency sweeps while the impulse train is running. The application shows a paid-out cable as a step between moves, which understates the problem, and the industrial measurements are the appropriate reference for what a fixed shaper loses under a real hoisting profile [12].

OPEN CHALLENGE Two Pendulums and a Moving Hoist

A crane with a heavy hook and a long attachment below it swings in a second significant mode, and feedback designed on a single pendulum can then destabilize a mode it never modeled. On an industrial overhead crane, both modes had to be identified, and the case of hoisting while the trolley moves, needed in practice, was left for future work [23]. A quay-crane study simply assumed that the operator never moves trolley and hoist together [4]. Progress would be a shaper or anti-sway loop that follows a live rope length through both modes.

Everything is planar. A bridge crane has a second horizontal axis, its own sway mode, a skew mode when the two axes are excited together, and load rotation about the cable. None of that is here, and a shaper that works on one axis in isolation has to be checked against the other before it goes on a machine.

The measurement chain is idealized in both directions. The trolley position carries no noise, no quantization and no delay, which makes the derivative term of Equation (12.14) better behaved than a real encoder and filter would allow. The swing angle is absent, or exact behind the predictive controller's sensor, rather than noisy, so the application cannot show what an angle measurement of realistic quality would buy, which is the comparison a design study would require.

The predictive controller's model omits the sine of the angle, worth 0.316° on the 14.14° unshaped swing, and treats every change to the hoist, payload, trolley or drive as model error, which is why it passes its swing limit on the long cable and loses the doubled payload.

Two smaller items are worth stating. The residual sway reported in Table 12.4 is a sampled amplitude rather than an integral, so a run whose trolley enters and leaves the parked band during an overshoot produces a residual number that depends on when it is read, and the 30 s horizon is stated because the force-limited fraction is a fraction of elapsed run time and shrinks as the run continues, which is why the application reports the time on the limit in seconds beside it. Neither affects any comparison made above, because every comparison is between runs read the same way over the same horizon.

12.9 Conclusion

This chapter studied an overhead crane simulation on five states. Four of them are mechanical and reach their accelerations through a two-by-two solve that is never linearized, and the fifth is the force the drive has actually developed. The plant is underactuated, with one drive force reaching both the trolley position and a payload resonance whose frequency depends on the cable length and on neither mass. The shipped controller is a single velocity-form proportional-integral-derivative loop on trolley position, above which the reference is convolved with a two-impulse or three-impulse train whose amplitudes are $[1, K]/(1+K)$ and $[1, 2K, K^2]/(1+K)^2$ at multiples of the damped half period, with $K = \exp(-\zeta_a \pi/\sqrt{1-\zeta_a^2})$ evaluated at an assumed cable length rather than the true one.

A fifth-order linearization places the closed-loop sway mode at a period of 3.8835 s against a measured 3.884 s, which is 3.3 % away from the $\sqrt{g/\ell}$ the shaper formulas use and therefore right at the edge of the two-impulse tolerance band. Thirteen configurations quantify the outcome, from a 6 m move that leaves 7.87° of residual sway unshaped and 0.30° with three impulses, to a doubled cable that costs a mistuned two-impulse shaper 44.6 % of the unshaped residual against the 43.7 % the sensitivity curve predicts, to a saturated drive on which shaping on and off give the same 7.7° peak. A model predictive controller given the shaper's cable length quiets the standard move 2.16 s sooner than three impulses with 55 % of the peak force, but loses on a longer cable and a doubled payload. A fuller simulator would add a double-pendulum hook block, concurrent hoisting, the second horizontal axis, and an instrumented swing angle with realistic noise so that command shaping and feedback anti-sway can be measured against each other on the same move. The application measures what an open-loop canceler is worth once its design frequency is no longer quite the frequency the plant has.

KEY POINTS

- One drive moves the trolley, and the load swings only through how the trolley speeds up and slows down, so the position loop cannot reach the swing.
- A shaped command splits each move into impulses a damped half period apart, so the later ones cancel the swing the first one starts.
- A shaper told 4 m on an 8 m cable leaves 44.6 % of the unshaped residual with two impulses and 19.9 % with three.
- A drive on its limit does not follow the shaped reference, and a shaper cannot remove sway already present.

Where else this applies. The same two-impulse and three-impulse shapers sit above the climber's speed loop in Volume 3, Chapter 12, where they cancel a structural mode of the ribbon rather than a swinging load.

References

[1] D. E. Seborg, T. F. Edgar, D. A. Mellichamp, and F. J. Doyle, III, *Process Dynamics and Control*, 4th ed. Hoboken, NJ: John Wiley & Sons, 2016.

[2] B. W. Bequette, *Process Control: Modeling, Design, and Simulation*. Upper Saddle River, NJ: Prentice Hall, 2003.

[3] K. J. Åström and R. M. Murray, *Feedback Systems: An Introduction for Scientists and Engineers*, 2nd ed. Princeton, NJ: Princeton University Press, 2021.

[4] E. Raubar and D. Vrančić, "Anti-sway system for ship-to-shore cranes," *Strojniški vestnik – Journal of Mechanical Engineering*, vol. 58, no. 5, pp. 338–344, 2012.

[5] W. Singhose, "Command shaping for flexible systems: A review of the first 50 years," *International Journal of Precision Engineering and Manufacturing*, vol. 10, no. 4, pp. 153–168, 2009.

[6] J. Vaughan, A. Yano, and W. Singhose, "Comparison of robust input shapers," *Journal of Sound and Vibration*, vol. 315, no. 4-5, pp. 797–815, 2008.

[7] O. J. M. Smith, "Posicast control of damped oscillatory systems," *Proceedings of the IRE*, vol. 45, no. 9, pp. 1249–1255, 1957.

[8] N. C. Singer and W. P. Seering, "Preshaping command inputs to reduce system vibration," *Journal of Dynamic Systems, Measurement, and Control*, vol. 112, no. 1, pp. 76–82, 1990.

[9] W. Singhose, W. Seering, and N. Singer, "Residual vibration reduction using vector diagrams to generate shaped inputs," *Journal of Mechanical Design*, vol. 116, no. 2, pp. 654–659, 1994.

[10] E. M. Abdel-Rahman, A. H. Nayfeh, and Z. N. Masoud, "Dynamics and control of cranes: A review," *Journal of Vibration and Control*, vol. 9, no. 7, pp. 863–908, 2003.

[11] L. Ramli, Z. Mohamed, A. M. Abdullahi, H. I. Jaafar, and I. M. Lazim, "Control strategies for crane systems: A comprehensive review," *Mechanical Systems and Signal Processing*, vol. 95, pp. 1–23, 2017.

[12] W. Singhose, L. Porter, M. Kenison, and E. Kriikku, "Effects of hoisting on the input shaping control of gantry cranes," *Control Engineering Practice*, vol. 8, no. 10, pp. 1159–1165, 2000.

[13] K. L. Sorensen, W. Singhose, and S. Dickerson, "A controller enabling precise positioning and sway reduction in bridge and gantry cranes," *Control Engineering Practice*, vol. 15, no. 7, pp. 825–837, 2007.

[14] Y. Fang, W. E. Dixon, D. M. Dawson, and E. Zergeroglu, "Nonlinear coupling control laws for an underactuated overhead crane system," *IEEE/ASME Transactions on Mechatronics*, vol. 8, no. 3, pp. 418–423, 2003.

[15] Y. Liu and H. Yu, "A survey of underactuated mechanical systems," *IET Control Theory & Applications*, vol. 7, no. 7, pp. 921–935, 2013.

[16] I. F. A. Vis and R. de Koster, "Transshipment of containers at a container terminal: An overview," *European Journal of Operational Research*, vol. 147, no. 1, pp. 1–16, 2003.

[17] A. Khalid, J. Huey, W. Singhose, J. Lawrence, and D. Frakes, "Human operator performance testing using an input-shaped bridge crane," *Journal of Dynamic Systems, Measurement, and Control*, vol. 128, no. 4, pp. 835–841, 2006.

[18] K. J. Åström and T. Hägglund, *Advanced PID Control*. Research Triangle Park, NC: ISA – The Instrumentation, Systems, and Automation Society, 2006.

[19] D. Q. Mayne, J. B. Rawlings, C. V. Rao, and P. O. M. Scokaert, "Constrained model predictive control: Stability and optimality," *Automatica*, vol. 36, no. 6, pp. 789–814, 2000.

[20] S. J. Qin and T. A. Badgwell, "A survey of industrial model predictive control technology," *Control Engineering Practice*, vol. 11, no. 7, pp. 733–764, 2003.

[21] H. Chen, Y. Fang, and N. Sun, "A swing constraint guaranteed MPC algorithm for underactuated overhead cranes," *IEEE/ASME Transactions on Mechatronics*, vol. 21, no. 5, pp. 2543–2555, 2016.

[22] G. Pannocchia and J. B. Rawlings, "Disturbance models for offset-free model-predictive control," *AIChE Journal*, vol. 49, no. 2, pp. 426–437, 2003.

[23] V. Helma and M. Goubej, "Active anti-sway crane control using partial state feedback from inertial sensor," in *2021 23rd International Conference on Process Control (PC)*. IEEE, 2021, pp. 137–142.

[24] T. R. Kuphaldt, *Lessons in Industrial Instrumentation*, version 2.33 ed. Open textbook, Creative Commons Attribution 4.0 license, ibiblio.org/kuphaldt/socratic/sinst, 2024.

[25] K. Stouffer, M. Pease, C. Tang, T. Zimmerman, V. Pillitteri, S. Lightman, A. Hahn, S. Saravia, A. Sherule, and M. Thompson, "Guide to operational technology (OT) security," National Institute of Standards and Technology, Gaithersburg, MD, Special Publication 800-82r3, 2023.

[26] Occupational Safety and Health Administration, "Overhead and gantry cranes, 29 CFR 1910.179," Code of Federal Regulations, Title 29, Chapter XVII, edition of July 1, 2024, U.S. Government Publishing Office, 2024. [Online]. Available: https://www.govinfo.gov/content/pkg/CFR-2024-title29-vol5/pdf/CFR-2024-title29-vol5-sec1910-179.pdf

12.10 Exercises

12.1 ⌕ Concept check · 2 min

The shipped controller of the crane is a velocity-form PID loop on trolley position with an input shaper above it. Scenario 9 starts the load swinging at 8° with the three-impulse shaper on and no move commanded. Which statement is right?

(a) The loop reads only the trolley position, so the shaper has nothing to act on and only the loop's coupling through the cable damps the swing

(b) The loop also reads the swing angle, so the three-impulse shaper cancels the initial swing within one damped half period

(c) The loop reads only the trolley position, but the shaper cancels the swing at its next impulse because its times follow the period

(d) The loop reads the cable tension, from which the shaper infers the swing and reshapes the setpoint to oppose it

12.2 ⌕ Concept check · 2 min

The first relation of Equation (12.1) is $(M+m)\ddot{x}+m\ell\ddot{\theta}\cos\theta-m\ell\dot{\theta}^2\sin\theta+b\dot{x}=F+W$. Which balance is it, and what trolley acceleration does a sudden drive force F produce with the load hanging still ($\theta=0$, $\dot{\theta}=0$, $\dot{x}=0$, $W=0$)?

(a) The moment balance on the payload about the pivot, and $F/(M+m)$

(b) The horizontal momentum balance on the trolley, and F/M

(c) The horizontal momentum balance on the trolley, and $F/(M+m)$

(d) The first-order lag of the drive force, and F/M

12.3 ⌕ Concept check · 2 min

Scenario 7 commands a 10 m move at $K_c=620\,\mathrm{N/m}$ on a drive rated at 1200 N. The peak sway is 7.70° with the two-impulse shaper and 7.73° without it. Why does the shaper do nothing here?

(a) The assumed cable length suits a 6 m move, so the impulses land out of phase on a 10 m move

(b) The two-impulse shaper is too sensitive to the frequency, and the three-impulse shaper would recover the cancellation

(c) The drive sits on its limit, so the trolley follows the force limit rather than the shaped reference

(d) The derivative filter delays the shaped command by more than one damped half period

12.4 Theory and calculation · 6 min

The shaper is set to its defaults, an assumed cable length $\ell_a = 4.00\,\text{m}$ and damping ratio $\zeta_a = 0.015$, with $g = 9.81\,\text{m/s}^2$.

(a) Find ω_n, T_n, ω_d and the decay factor K of Equation (12.10). *Checkpoint:* $\omega_n = 1.5660\,\text{rad/s}$, $T_n = 4.012\,\text{s}$, $K = 0.9540$.

(b) Find the amplitudes and times of the two-impulse and the three-impulse shapers. *Checkpoint:* 0.5118 and 0.4882 at 0 and 2.006 s; 0.2619, 0.4997 and 0.2384 at 0, 2.006 and 4.013 s.

(c) The assumed length is set to 8.00 m. Find the new half period and the delay of the three-impulse shaper, and say which amplitudes change. *Checkpoint:* 2.837 s and 5.67 s; no amplitude changes.

12.5 Theory and calculation · 6 min

The position loop is approximately the second-order system of Equation (12.6), with $M + m = 1350\,\text{kg}$ and $b = 400\,\text{N s/m}$.

(a) Find ω_c and ζ_c at the default tuning, $K_c = 620\,\text{N/m}$ and $\tau_D = 2.3\,\text{s}$, and the ratio of the sway frequency 1.566 rad/s to ω_c. *Checkpoint:* 0.678 rad/s, 1.00, 2.3.

(b) The challenge loads $K_c = 300\,\text{N/m}$ and $\tau_D = 0.5\,\text{s}$, and suggests 660 N/m and 2.5 s. Find ζ_c for both, and the overshoot that a second-order loop predicts for the first. *Checkpoint:* 0.43 and 1.09; about 22 %.

(c) Find the gain that would place ω_c at twice the sway frequency, and the force it would ask for on a 6 m step. *Checkpoint:* 13.2 kN/m and 79 kN.

12.6 Theory and calculation · 5 min

For an undamped mode, Section 1.4.8 gives the residual of a two-impulse shaper as $|\cos(\pi r/2)|$ of the unshaped residual and that of a three-impulse shaper as $\cos^2(\pi r/2)$, where r is the ratio of the true to the design frequency.

(a) The cable is 8 m and the shaper is told 4 m. Find r and both residual fractions, and compare them with the 43.7 % and 19.1 % of Equation (12.9) with damping. *Checkpoint:* $r = 0.707$; 44.4 % and 19.7 %.

(b) Find the band of r that keeps each residual at or below 5 %, and the ratio of the band widths. *Checkpoint:* 0.968 to 1.032 and 0.856 to 1.144; a ratio of 4.5.

12.7 App challenge · 8 min

Load scenario 1, *Fast move, shaping off*, at the default seed and change nothing. Run to $t = 30\,\text{s}$ and pause. Then do the same in scenario 2, *ZV input shaping*, and scenario 3, *ZVD input shaping*. After each run, read the Peak sway and Shaper delay tiles and export the CSV.

(a) In scenario 1, read the Peak sway tile and the column `sway_amplitude_deg` at $t = 20\,\text{s}$ (tolerance 0.02°). *Checkpoint:* 14.14° and 2.81°.

(b) Read the same two values and the Shaper delay tile in scenarios 2 and 3. *Checkpoint:* 6.29°, 0.26°, 2.01 s; 3.23°, 0.07°, 4.01 s.

(c) The shaper is given the true 4.00 m cable in both runs. Explain why three impulses leave about a quarter of the amplitude of two at 20 s. *Checkpoint:* The true mode sits 3.3 % above the design frequency.

12.8 App challenge · 9 min

Load scenario 7, *Drive force saturation (10 m on a 1200 N drive)*, at the default seed. It starts with the two-impulse shaper on and $K_c = 620\,\text{N/m}$. Each run lasts 30 s; read the Peak sway and Force limited tiles at the end (tolerance 0.02° and 0.05 s).

(a) Run the scenario as loaded. *Checkpoint:* 7.70°; 3.04 s (10.1 %).

(b) Press Reset, set Input shaper to OFF before Run, and run again. *Checkpoint:* 7.73°; 3.45 s (11.5 %).

(c) Reload the scenario, set Proportional gain to 60 N/m before Run and run with the shaper on. Then press Reset, set Input shaper to OFF and run again. Explain the four results. *Checkpoint:* 1.82° and 3.56°, with 0.00 s on the limit.

12.9 App challenge · 9 min

Load the challenge, *Challenge, park an 8 m move quietly*, at the default seed. It is judged at $t = 30$ s: from 20 s on the trolley must stay within 0.10 m of 8 m with a sway amplitude under 1.0°, and the drive must spend no time on its limit. A failed run is reported in the progress checklist with its worst position error, worst sway amplitude and force-limited share. Make every change before Run, press Reset between runs and leave the suggested tuning hidden.

(a) Run as loaded to 30 s. Which targets fail, and by how much? *Checkpoint:* 0.14 m and 4.32°; the force target is met.

(b) Set Derivative time to 2.5 s and Proportional gain to 660 N/m, leave the shaper OFF, and run again. Read the checklist and the Peak sway and Force limited tiles. *Checkpoint:* 0.05 m, 3.85°, 0.5 %; 18.55° and 0.16 s.

(c) Set Input shaper to ZVD and run again. Read the Peak sway and Force limited tiles, and the largest `sway_amplitude_deg` from 20 s on in the exported file (tolerance 0.02°). *Checkpoint:* 4.26°, 0.00 s, 0.16°; the challenge is met.

12.10 Application area · 4 min

A container terminal counts crane moves per hour, and an operator does not lower a load until its swing is below about 0.5°. The unshaped 6 m move of scenario 1 parks at 9.88 s with 7.87° of sway, and the closed loop decays the amplitude with a time constant of 10.38 s.

(a) Estimate when the load becomes quiet, and compare with the three-impulse shaper, which parks at 12.72 s with 0.30°. *Checkpoint:* About 38.5 s; about 26 s longer.

(b) Derating the drive to 1400 N cuts the unshaped residual to 5.36°. Say why an operator who slows the crane this way pays more than the shaper costs. *Checkpoint:* Move time on every cycle, and the load still has to be waited for.

12.11 Application area · 3 min

An outdoor gantry crane carries the default 150 kg load in a steady 120 N wind along the rail, as in scenario 11.

(a) Find the angle at which the load hangs, and say whether a shaper or a retuned position loop can bring it back to vertical. *Checkpoint:* 4.662°; neither can.

(b) The position loop runs proportional-derivative only. Find the steady offset of the trolley, and say what removes it. *Checkpoint:* About 0.194 m; integral action.

12.12 Review the agent · 5 min

An AI assistant is asked to commission the shaper on the default crane and replies: “The swing frequency of a hanging load is $\sqrt{g/\ell}$ and holds neither mass, so set Shaper cable length to exactly the true 4.00 m. Any other setting can only add residual sway. Use two impulses, since three add a needless 2 s.” Find the flaw, and say how to check it in the app.